

# Electrochemical Study on Mixture of 1M LiPF<sub>6</sub> and Carbonate Solvents as an Electrolyte in Graphite/ Lithium and Graphene/ Lithium-Ion Batteries

Tongxia Wu

Office of Quality Management, Guangxi Polytechnic of Construction, NanNing 530007, China  
E-mail: [wtx0546@126.com](mailto:wtx0546@126.com)

Received: 15 August 2022 / Accepted: 15 September 2022 / Published: 20 October 2022

The fabrication of graphite/Li and graphene/Li cells, electrochemical characterization of these cells, and assessment of a mixture of 1M LiPF<sub>6</sub> and carbonate solvents (ethylene carbonate (EC), diethyl carbonate (DEC), dimethyl carbonate (DMC), ethyl methyl carbonate (EMC), sulfolane (SL), and fluoroethyl carbonate (FEC)) were the main topics of this study. According to morphological studies, graphene had a far larger effective surface area and porosity than graphite. According to electrochemical tests utilizing CV and EIS techniques, graphene had a higher storage capacity than ultra-thin graphite. The researchers found that graphene has excellent rate capability and can facilitate charge transfer during discharge-charge actions. Study charge/discharge profiles at the current density of 200 mA g<sup>-1</sup> in the electrolyte of 1M LiPF<sub>6</sub> containing EMC/EC/DEC/DMC with a volume ratio of 1:1:5:2 (1M LiPF<sub>6</sub> + (EMC/EC/DEC/DMC 1:1:5:2)) as optimal stoichiometry of EC, DEC, DMC, EMC solvents showed that for graphite, the first-cycle discharge and charge capacities were 138 and 111 mAh g<sup>-1</sup>, respectively, and for graphene, the corresponding capacities were enhanced to 143 and 117 mAh g<sup>-1</sup> respectively. Moreover, results showed graphene electrode in graphene/Li cell using 1M LiPF<sub>6</sub> containing (EMC/EC/DEC/DMC/SL 1:1:5:2:1) and (EMC/EC/DEC/DMC/FEC 1:1:5:2:1) showed that excellent specific capacity more than 124 mAh g<sup>-1</sup> and good stability over 500 cycles were obtained for electrolyte solution containing EMC/EC/DEC/DMC/SL with volume ratio of 1:1:5:2:1, and the SL-mixed solution can be employed at high potential (5.3 V vs Li/Li<sup>+</sup>).

**Keywords:** Carbonate solvent; Lithium-ion batteries; Graphite/Li cells; Graphene/Li cells

## 1. INTRODUCTION

Electronics, toys, wireless headphones, handheld power tools, small and big appliances, electric cars, and electrical energy storage devices all employ lithium-ion (Li-ion) batteries [1, 2]. In a Li-ion battery, Li<sup>+</sup> ions flow from the negative electrode to the positive electrode through an electrolyte during discharge and return when charging [3, 4]. The positive electrode was made of an intercalated

lithium compound, whereas the negative electrode is usually made of graphite [5]. In a Li-ion battery, the electrolyte is the liquid that allows electrical current to pass between the anode and the cathode [6, 7]. Electrolytes can be in the form of liquids or solids. Electrolytes are typically soluble salts, acids, and bases [8, 9].

Meanwhile, there are certain issues with Li-ion batteries, which may be traced back to the fact that extracting the raw elements, primarily lithium and cobalt, consumes a lot of energy and water [10, 11]. Another issue with Li-ion batteries is that they are not suitable for use in high temperature environments [12, 13]. The use of Li-ion batteries in cellphones and high-temperature electronic gadgets is restricted [14]. The problem with employing liquid electrolytes in Li-ion batteries is that they decompose [15, 16]. Using too much electrolyte in Li-ion batteries causes more volatile materials to decompose and form a thicker solid electrolyte interphase layer on the electrode surface, especially at relatively high temperatures, resulting in a decrease in the battery's specific energy and energy density due to the electrolyte's dead weight [17, 18].

Many studies have been conducted to resolve these issues by studying the electrochemical behaviors and thermal stability of Li-ion batteries composed of various composite and hybrid materials for electrodes, such as mesoporous  $\text{Co}_3\text{O}_4$  nanosheets-3D graphene [19], carbon nanotube/graphene hybrid materials [20, 21],  $\text{NiFe}_2\text{O}_4$ -Coated Activated Carbon Composite [22], core-shell structure  $\text{TiO}_2@$  TiN spheres [23], etc. Finding suitable electrolytes for lithium batteries is urgently needed [24], and thereby gel polymer electrolytes [25], ionic liquids [26] and organic electrolytes [27] have been investigated in high temperature and high voltage conditions. Organic electrolytes are preferred over aqueous electrolytes in Li-ion batteries because the organic electrolyte solution can be replaced with a non-flammable aqueous electrolyte with high ionic conductivity (about 2 orders of magnitude higher than organic electrolytes), resulting in good rate performance and low over potentials [28, 29]. Despite the fact that different materials are being investigated, The electrochemical performance of Li-ion batteries still rely on  $\text{LiPF}_6$  dissolved in carbonate solvents such as ethylene carbonate (EC), diethyl carbonate (DEC), dimethyl carbonate (DMC), and ethyl methyl carbonate (EMC) [30, 31]. This is necessary for determining the optimal stoichiometry of these solvents in order to optimize the performance of Li-ion batteries. As a result, the focus of this research was on the manufacturing and electrochemical characterization of graphite/Li and graphene/Li cells, as well as the evaluation of carbonate solvents (EC, DEC, DMC, EMC) as Li-ion battery electrolytes. The coin type graphite/Li and graphene/Li cells were fabricated using a mixture of PVDF and graphite and graphene powders, respectively, and  $\text{LiPF}_6$  was used as the electrolyte solution. In order to optimize the carbonate solvents in electrolyte solution, 1M  $\text{LiPF}_6$  containing EC as control, EMC/EC with volume ratio of 1:1 (EMC/EC 1:1), (EMC/EC/DMC 1:1:1), (EMC/EC/DEC 1:1:1), (EMC/EC/DEC/DMC 1:1:1:1), (EMC/EC/DEC/DMC 1:1:1:2), (EMC/EC/DEC/DMC 1:1:2:1) and (EMC/EC/DEC/DMC 1:1:5:2), (EMC/EC/DEC/DMC/ SL 1:1:5:2:1) and (EMC/EC/DEC/DMC/ FEC 1:1:5:2:1) were electrochemically characterized.

## 2. EXPERIMENT

### 2.1. Fabrication the coin type graphite/Li and graphene/Li cells

The coin type graphite/Li and graphene/Li cells (CR2032) consist of a positive cathode and a lithium metal negative electrode, and separators were fabricated as follows: First, graphite electrode was prepared by mixing 8 mg of graphite powder (99%, Shandong Carbon Lide Nano Material Co., Ltd., China) and 1 mg of poly(vinylidene fluoride) (PVDF, 99.9%, Xiamen Tob New Energy Technology Co., Ltd., China). For the preparation of the graphene electrode, the same process was performed using graphene powder (Sigma-Aldrich). The mixture was coated onto an aluminum mesh (Hebei Chaochuang Metal Mesh Co., Ltd., China) and the composite electrode was dried in a convection oven at 100 °C for 100 minutes before use. 250  $\mu$ L of the electrolyte solution was prepared ultrasonically adding a commercially 1.0 M lithium hexafluoro phosphate (LiPF<sub>6</sub>, 99%, Shanghai Talent Chemical Co., Ltd., China) ultrasonically added in a solvent mixture of ethylmethyl carbonate (EMC, 99%, Sigma-Aldrich) and ethylene carbonate (EC, 98%, Sigma-Aldrich) with a 1:1 volume ratio. Then, dimethyl carbonate (DMC,  $\geq$ 99%) and diethyl carbonate (DEC, 99%), sulfolane (SL, 99%, Sigma-Aldrich) and fluoroethyl carbonate (FEC, 99%, Sigma-Aldrich) were added into the electrolyte. The prepared electrolytes in this study were 1M LiPF<sub>6</sub> containing EC, EMC/EC with a volume ration of 1:1 (EMC/EC 1:1), (EMC/EC/DMC 1:1:1), (EMC/EC/DEC 1:1:1), (EMC/EC/DEC/DMC 1:1:1:1), (EMC/EC/DEC/DMC 1:1:1:2), (EMC/EC/DEC/DMC 1:1:2:1) and (EMC/EC/DEC/DMC 1:1:5:2), (EMC/EC/DEC/DMC/ SL 1:1:5:2:1) and (EMC/EC/DEC/DMC/ FEC 1:1:5:2:1). Lithium-foil (Shandong AME Energy Co., Ltd., China) was used as the counter electrode. Two pieces of glass fiber filter are used as separators (GMFs, Whatman). The coin cell was assembled in an argon-filled glove box (Mikrouna, Super 1220/750/900, China).

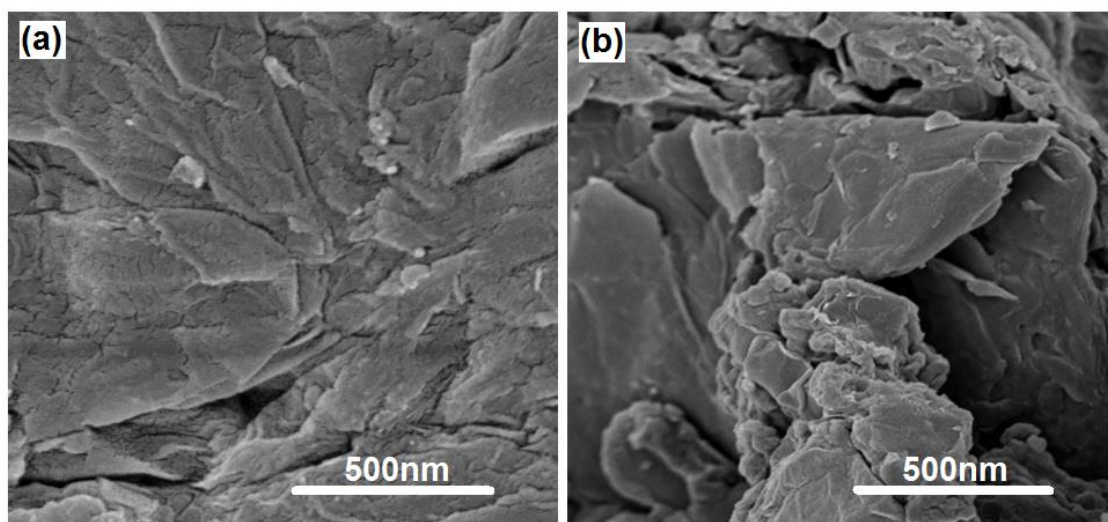
### 2.2. Measurements

Electrochemical experiments were conducted on galvanostatic charge-discharge cycling between 3 V and 5.2 V vs. Li<sup>0</sup>/Li<sup>+</sup> at a current density of 50mA g<sup>-1</sup> on a Mac-Pile battery tester at room temperature. The electrochemical impedance spectroscopy (EIS) experiments were carried out using the ZENNIUM electrochemical workstation (ZAHNER-elektrok GmbH & Co. KG, Germany). Prior to the EIS experiments, two graphite electrodes (or graphene electrodes) were charged to 5.2 V vs. Li<sup>0</sup>/Li<sup>+</sup> and then assembled in each symmetric cell. At open circuit, EIS measurements were taken at amplitude of 5 mV in the frequency range of 10<sup>5</sup> Hz to 10<sup>-2</sup> Hz at open circuit. Gas chromatography (Thermo Scientific, Waltham, USA) equipped with an Acclaim™ 120 column (C18, 4.6 × 250 mm, Thermo Scientific) was applied to the analysis of the electrolytes. The flow rate of helium, injection volume and temperature were 1 ml/min, 5  $\mu$ l and 245 °C, respectively. The morphology and structure of the samples were analyzed by a scanning electron microscope (SEM, Hitachi S-4700, Japan).

### 3. RESULTS AND DISCUSSION

#### 3.1. Analyses of morphology

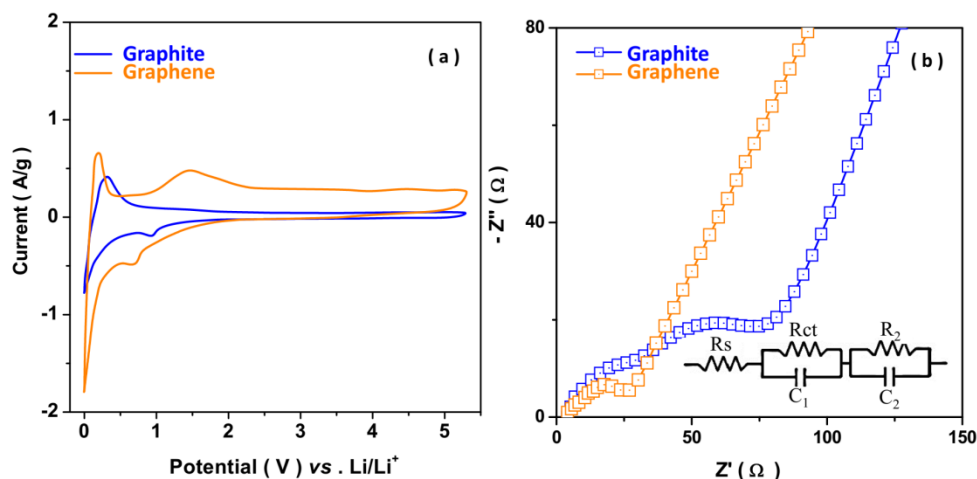
Figures 1a and 1b show SEM images of graphite and graphene, respectively. Figure 1a displays a porous and twisted graphite morphology that exfoliated into ultrathin sheets with wavy patterns. SEM photos of graphene show crumpled graphene oxide nanosheets with a shape similar to heavily wrinkled paper that ripple and entangle with one another. These photos show that graphene has a higher porosity and a far larger effective surface area than graphite.



**Figure 1.** SEM images of (a) graphite and (b) graphene.

#### 3.2. Electrochemical analyses

Figure 2a shows the CV curve of the first cycle for graphite and graphene at voltages ranging from 0 to 5.3V (vs.  $\text{Li}/\text{Li}^+$ ) in 1M  $\text{LiPF}_6$  containing (EMC/EC/DEC/DMC 1:1:5:2), revealing characteristic peaks due to  $\text{Li}^+$  ion intercalation/deintercalation with graphitic layers [32-34]. Storage of Li in graphite and graphene can be attributed to Faradaic charge transfer processes between the electrolyte species and the carbon nanostructures' edges or surface locations in this potential window [33, 35, 36]. It has been discovered that ultra-thin graphite has the lowest storage capacity, whereas graphene has a high storage capacity due to its large effective surface area and good ability to reactivity with the electrolyte to chemisorb  $\text{Li}^+$  ions [33, 37].



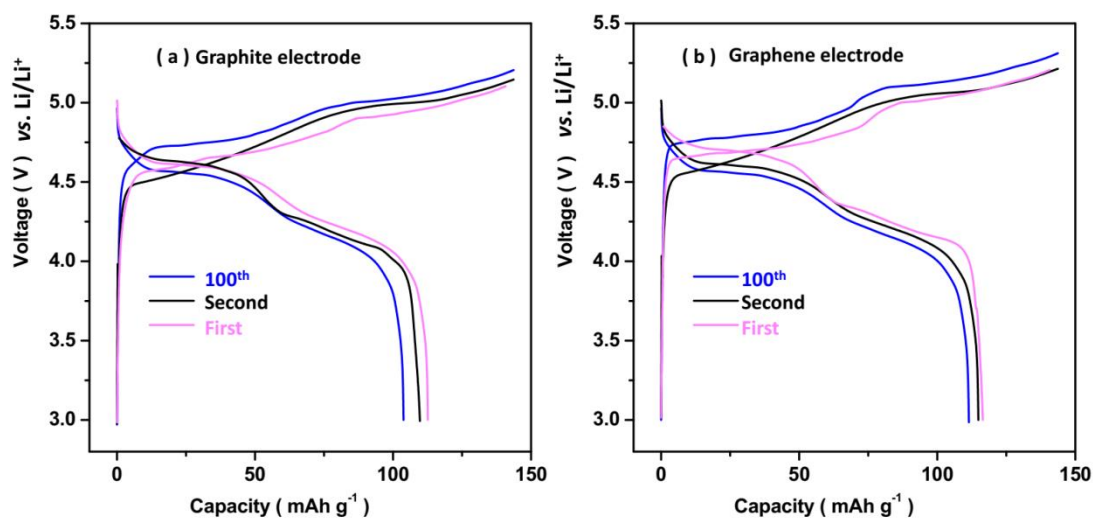
**Figure 2.** (a) CV curve of first cycle at voltages from 0–5.3 V (vs. Li/Li<sup>+</sup>) for graphite and graphene at scan rate of 1 mV/s. (b) Nyquist plots of graphite and graphene electrodes after 100 discharge-charge cycles at 100 mA g<sup>-1</sup>, and the equivalent circuit model.

Figure 2b depicts EIS spectra of graphite and graphene electrodes after 100 discharge-charge cycles at 200 mA g<sup>-1</sup> in 1M LiPF<sub>6</sub> containing (EMC/EC/DEC/DMC 1:1:5:2). The resulted Nyquist plots contains two semicircles that the first semicircle demonstrated to migration resistance Li<sup>+</sup> ion through the solid electrolyte interphase films (R<sub>2</sub>), and second semicircle related to resistance of charge transport (R<sub>ct</sub>) [38, 39]. Moreover, the related equivalent circuit is presented in Figure 2b also consists of R<sub>s</sub> as the resistance of electrolyte. The obtained values for parameters by fitting the curves using ZView software are given in Table 1. The results show R<sub>ct</sub> of the graphene electrode is smaller than graphite, implying that graphene can facilitate charge transfer process during discharge-charge actions and provide excellent rate capability [38, 40, 41].

**Table 1.** Obtained parameter by fitting data according to the equivalent circuit model.

Sample	R <sub>s</sub> (Ω)	R <sub>ct</sub> (Ω)	R <sub>2</sub> (Ω)
Graphene	2.83	10.6	9.78
Graphite	2.91	44.11	28.91

Figure 3 exhibits the voltage profile of the first, second and 100<sup>th</sup> charge–discharge cycles of graphite and graphene electrodes vs. Li/Li<sup>+</sup> at the current density of 200 mA g<sup>-1</sup> in 1M LiPF<sub>6</sub> containing (EMC/EC/DEC/DMC 1:1:5:2). Typical Li<sup>+</sup> insertion/extraction profiles are observed for both electrodes. Comparison between the profiles displays a larger charge/discharge voltage hysteresis for the graphene electrode. For graphite, the first-cycle discharge and charge capacities are 138 and 111 mAh g<sup>-1</sup>, respectively, and for graphene, the corresponding capacities are enhanced to 143 and 117 mAh g<sup>-1</sup> respectively.



**Figure 3.** Voltage profile of the first, second and 100<sup>th</sup> charge–discharge cycles of (a) graphite and (b) graphene electrodes vs. Li/Li<sup>+</sup> at the current density of 200 mA g<sup>-1</sup> in 1M LiPF<sub>6</sub> containing (EMC/EC/DEC/DMC 1:1:5:2).

This enhancement in capacity can be related to nanopores, curled morphology edge-type sites as active defects, and the larger effective surface area of graphene nanosheets as disordered carbon nanostructures, which provide more Li<sup>+</sup> insertion active sites. In the second cycle, the specific capacity of graphene decreased to 115 mAh g<sup>-1</sup>, but it is maintained at 112 mAh g<sup>-1</sup> in the 100<sup>th</sup> cycle. These observations illustrate the stable cyclic performance of graphene from the second cycle due to formation of stable solid electrolyte interphase film during the first discharge process [42-44]. Furthermore, studies have shown that, when compared to graphene materials, graphite materials have a higher c-axis thickness and require more activation energy to extend the interlayer spacing between adjacent layers, resulting in slower ion kinetics [45, 46].

Figure 4 shows first-cycle galvanostatic charge/discharge curves versus specific energy of graphene electrode during cell cycling in situ at 200 mA g<sup>-1</sup> in 1M LiPF<sub>6</sub> containing (EC), (EMC/EC 1:1), (EMC/EC/DMC 1:1:1), (EMC/EC/DEC/DMC 1:1:1:1), (EMC/EC/DEC/DMC 1:1:1:2), (EMC/EC/DEC/DMC 1:1:2:1), (EMC/EC/DEC/DMC 1:1:5:2) and (EMC/EC/DEC/DMC 1:1:6:2) as electrolyte solutions. It is found that the graphene electrode shows extremely low reversible capacity less than 20 mAh g<sup>-1</sup> in the 1M LiPF<sub>6</sub> containing EC (15 mAh g<sup>-1</sup>) and (EMC/EC 1:1) (19 mAh g<sup>-1</sup>) solutions, which is far less than the obtained value (100 mAh g<sup>-1</sup>) by Fan et al. [47] in 1M LiPF<sub>6</sub>-EMC. The differences in the activity of lithium-based cells using cyclic and linear carbonate-based electrolyte solutions indicated that EMC can facilitate and delicately tune the intercalation behavior of solvated PF<sub>6</sub><sup>-</sup> into graphene electrodes [48, 49]. Therefore, this condition may result in the activity of physical mixtures of DEC and DMC in the LiPF<sub>6</sub> solutions being similar to the chemical hybrid of EMC, and remarkably enhancing the graphene electrode performance. As depicted in Figure 4, the first cycle discharge capacity increased from 29.2 mAh g<sup>-1</sup> (LiPF<sub>6</sub>+ EMC/EC/DMC 1:1:1) to 115 (LiPF<sub>6</sub>+EMC/EC/DEC/DMC 1:1:6:2) and 117 mAh g<sup>-1</sup> (LiPF<sub>6</sub>+EMC/EC/DEC/DMC 1:1:5:2) with the addition of the mixture and DEC content in solution. This observation indicates that the nature of the alkylcarbonate mixture plays an important role in the stabilization/destabilization of the electrode–

electrolyte interphase [50]. In addition, it has been suggested that the mixture solvent of DMC/DEC can provide higher conductivity as compared to the DMC and DEC electrolyte because DMC/DEC itself has a higher degree of ionic dissociation than DMC and DEC [51, 52].

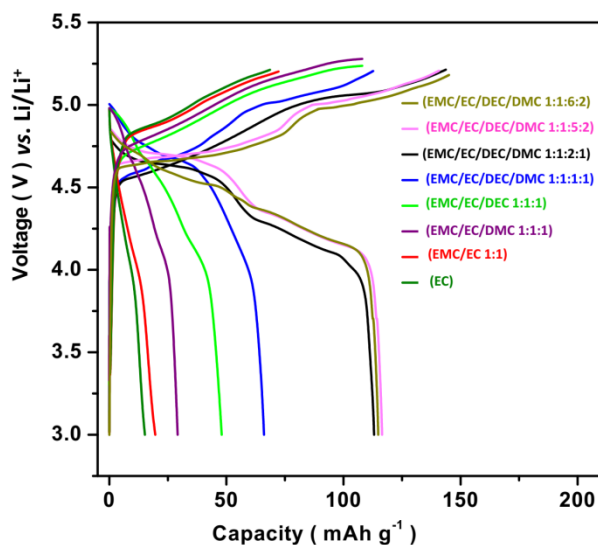


**Figure 4.** First-cycle galvanostatic charge/discharge curves versus specific energy of graphene electrode during cell cycling in situ, graphene/Li cells at charge-discharge rate of  $200 \text{ mA g}^{-1}$  in different electrolytes electrolyte solutions.

Figure 5 shows the cycling performance of the graphene/Li cells using  $1 \text{ M LiPF}_6$  containing (EMC/EC/DEC/DMC 1:1:1:1), (EMC/EC/DEC/DMC 1:1:1:2), (EMC/EC/DEC/DMC 1:1:2:1), (EMC/EC/DEC/DMC 1:1:5:2) and (EMC/EC/DEC/DMC 1:1:6:2) as electrolyte solutions at charge-discharge rate of  $200 \text{ mA g}^{-1}$  in the potential range from 3 V to 5.2 V. As depicted, the electrolyte EMC/EC/DEC/DMC with volume ratio of 1:1:5:2 presents the optimal cycling performance with great initial capacity ( $117 \text{ mAh g}^{-1}$ ) for first cycle, then decreased to around  $111 \text{ mAh g}^{-1}$  in 12<sup>th</sup> cycle, and then increased up  $116 \text{ mAh g}^{-1}$  and prolonged cycling stability after 500 cycles which are in agreement with the results of  $1 \text{ M LiPF}_6$ -EMC [47, 53]. Ethylene and diethyl carbonates serve as double-edged sword in graphene/Li cells, demonstrating the great protecting effect toward the graphene electrode because of formation solid electrolyte interphase at the graphene/electrolyte interface [24]. Moreover, it is suggested that in the charge/discharge process, the  $\text{PF}_6^-$  anions in the electrolyte are absorbed/desorbed on the surface of graphitic electrode and simultaneously  $\text{PF}_6^-$  anion intercalation/de-intercalation process occurs on graphene based electrode for charge storage/delivery [54], and ethyl group may create solvation shell around  $\text{PF}_6^-$  anion than that methyl group [55], indicating to charge/discharge process without exfoliation. As seen, all electrolyte solutions exhibit excellent capacity retention for the first 500 cycles at a rate of  $200 \text{ mA g}^{-1}$ . As observed, it attains more than 94%, 94%, 98%, 99% and 99% for electrolyte solutions of  $1 \text{ M LiPF}_6$  containing (EMC/EC/DEC/DMC 1:1:1:1), (EMC/EC/DEC/DMC 1:1:1:2), (EMC/EC/DEC/DMC 1:1:2:1), (EMC/EC/DEC/DMC 1:1:5:2) and (EMC/EC/DEC/DMC 1:1:6:2), respectively. The most stable cycling performance and the highest discharge capacity over 500 cycles are obtained on the electrolyte

1M LiPF<sub>6</sub> containing EMC/EC/DEC/DMC with a volume ratio of 1:1:5:2. Therefore, this electrolyte solution was selected for further studies.

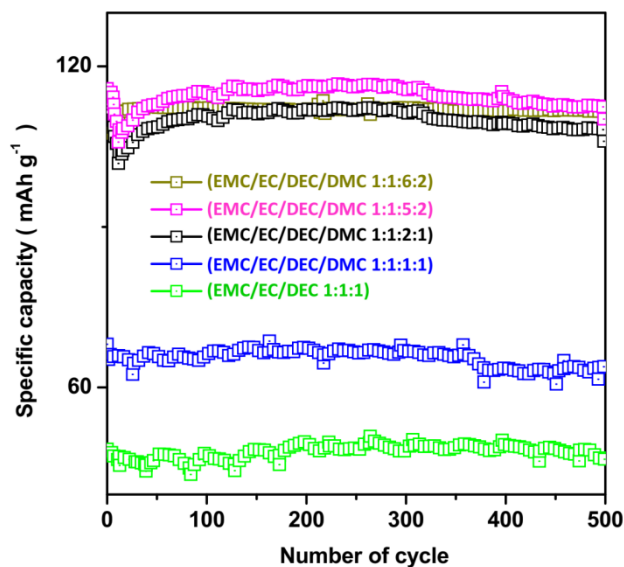
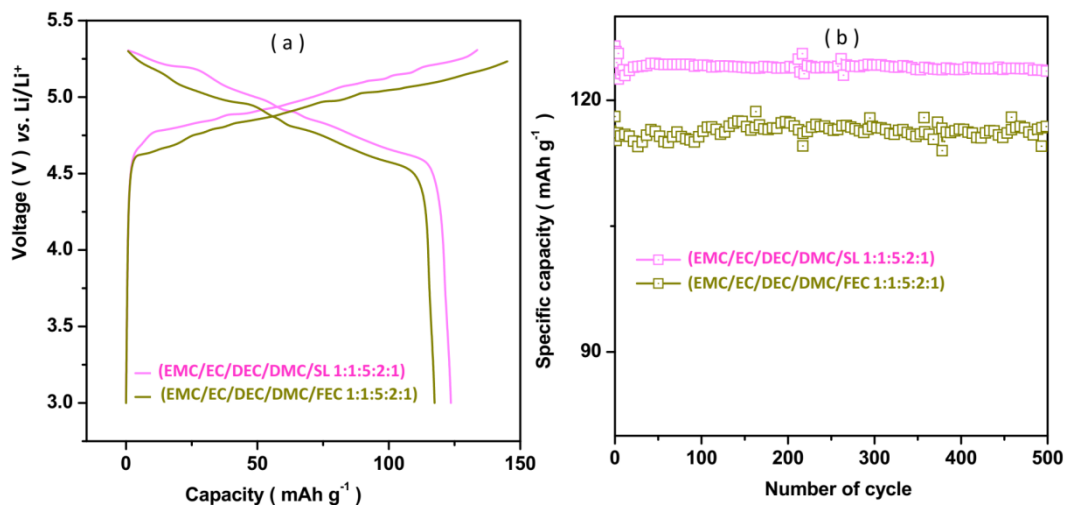


**Figure 5.** The specific capacity vs. cycle number is reported, for the first 500 cycles of the graphene/Li cells using 1M LiPF<sub>6</sub> containing (EMC/EC/DEC/DMC 1:1:1:1), (EMC/EC/DEC/DMC 1:1:1:2), (EMC/EC/DEC/DMC 1:1:2:1), (EMC/EC/DEC/DMC 1:1:5:2) and (EMC/EC/DEC/DMC 1:1:6:2) as electrolyte solutions at charge-discharge rate of 200 mA g<sup>-1</sup> in the potential range from 3 V to 5.2 V.

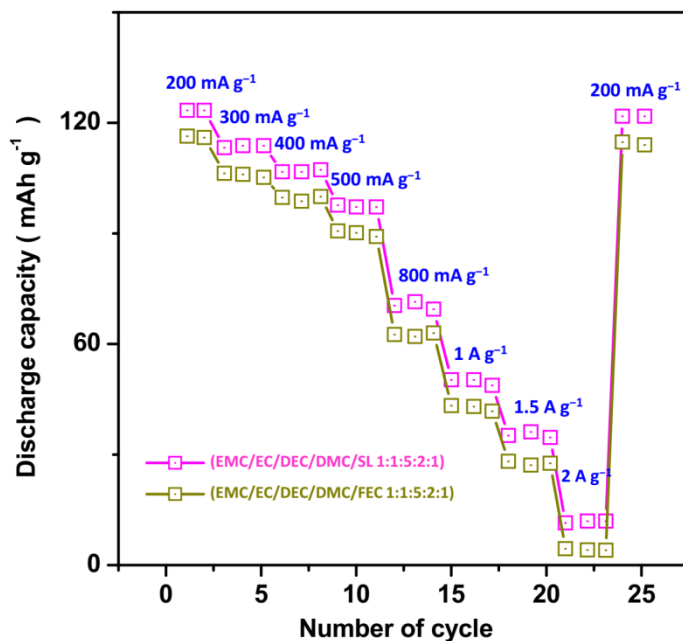
Figures 6a and 6b show the first galvanostatic charge-discharge curves and the cycling performances of graphene electrodes in graphene/Li cells using 1M LiPF<sub>6</sub> containing (EMC/EC/DEC/DMC/SL 1:1:5:2:1) and (EMC/EC/DEC/DMC/FEC 1:1:5:2:1) electrolyte solutions. It is found that excellent specific capacity of more than 124 mAh g<sup>-1</sup> and good stability over 500 cycles are obtained for electrolyte solution containing EMC/EC/DEC/DMC/SL with a volume ratio of 1:1:5:2:1, and the SL-mixed solutions can be employed at a high potential (5.3 V vs Li/Li<sup>+</sup>).

Figure 7 exhibits the rate capability of the graphene electrode in a graphene/Li cell using 1M LiPF<sub>6</sub> containing (EMC/EC/DEC/DMC/SL 1:1:5:2:1) and (EMC/EC/DEC/DMC/FEC 1:1:5:2:1) at a rate range from of 200 mA g<sup>-1</sup> to 2 A g<sup>-1</sup> for 25 cycles in the wide voltage range from 3 to 5.3 V at 65 °C to evaluate the high temperature and high voltage effects. It has been discovered that the electrolyte containing (EMC/EC/DEC/DMC/SL 1:1:5:2:1) as solvent has a higher discharge capacity toward the electrolyte containing (EMC/EC/DEC/DMC/FEC 1:1:5:2:1). Moreover, as seen, the discharge capacity of the graphene electrode is 25mAh g<sup>-1</sup> at 2A g<sup>-1</sup>. That concordances to 20% of the capacity at 200 mA g<sup>-1</sup> (124 mAh g<sup>-1</sup>). In addition, after various rates cycles, the capacities of the graphene electrode are recovered to their initial levels when current rate returns to 200 mA g<sup>-1</sup>, indicating that there is no structural damage to the layer structure at high current and fast rates [45, 56]. The results demonstrate the great potential of efficient performance of graphene materials for batteries in 1M LiPF<sub>6</sub> containing (EMC/EC/DEC/DMC/SL 1:1:5:2:1) at high temperature and high voltage conditions which is also confirmed by density functional theory (DFT) calculations [57, 58]. Table 2

shows the comparison between the electrochemical performance of graphene/Li cell using 1M LiPF<sub>6</sub> containing (EMC/EC/DEC/DMC/SL 1:1:5:2:1) and various reported Li ion battery cells which indicate better or comparable performance of graphene/Li.



**Figure 6.** (a) The first galvanostatic charge-discharge curves and (b) the cycling performances of graphene electrode in graphene/Li cell using 1M LiPF<sub>6</sub> containing (EMC/EC/DEC/DMC/SL 1:1:5:2:1) and (EMC/EC/DEC/DMC/FEC 1:1:5:2:1) electrolyte solutions at 200 mA g<sup>-1</sup>.



**Figure 7.** Rate capability of graphene electrode in graphene/Li cell using 1M LiPF<sub>6</sub> containing (EMC/EC/DEC/DMC/SL 1:1:5:2:1) and (EMC/EC/DEC/DMC/FEC 1:1:5:2:1) at a rate range from of 200 mA g<sup>-1</sup> to 2 A g<sup>-1</sup> for 25 cycles in the wide voltage range from 3 to 5.3 V at 60 °C.

**Table 2.** Comparison between the electrochemical performance of graphene/Li cell using 1M LiPF<sub>6</sub> containing (EMC/EC/DEC/DMC/SL 1:1:5:2:1) and various reported Li ion battery cells.

Composition	voltage range (V)	Electrolyte	Discharge capacity	Capacity retention (%)	Ref.
graphene	3–5.3	1M LiPF <sub>6</sub> + (EMC/EC/DEC/DMC/SL 1:1:5:2:1)	124 (200 mA g <sup>-1</sup> )	99% (500 cycles) at 200 mA g <sup>-1</sup>	This study
		1M LiPF <sub>6</sub> + (EMC/EC/DEC/DMC/FEC 1:1:5:2:1)	117 (200 mA g <sup>-1</sup> )	99% (500 cycles) at 200 mA g <sup>-1</sup>	
Graphite	3–5.2	1M LiPF <sub>6</sub> +EMC	104 (200 mA g <sup>-1</sup> )	71% (500 cycles) at 200 mA g <sup>-1</sup>	[47]
		1M LiPF <sub>6</sub> +EC	80 (200 mA g <sup>-1</sup> )		
Graphite	3.6–4.2	1M LiPF <sub>6</sub> +(EC/EMC 3:7)	102 (0.5 mA cm <sup>-2</sup> )	75% (200 cycles) at 0.5 mA cm <sup>-2</sup>	[59]
LiFePO <sub>4</sub> /artificial graphite	1.7–2.0	1M LiPF <sub>6</sub> + (EC/PC/ DMC 1:1:3)	376 mAh (0.5 C)	90.8% (100 cycles) at 0.5 C	[60]
Graphite	0.025–1.5	1M LiPF <sub>6</sub> + (EC /DEC 1:1)	370 (1 C)	99% (100 cycles) at 1 C	[61]

#### 4. CONCLUSION

The focus of this research was on the manufacture and electrochemical characterization of graphite/Li and graphene/Li cells, as well as the evaluation of a mixture of carbonate solvents (EC, DEC, DMC, EMC, SL, and FEC) as a Li-ion battery electrolyte. SEM investigation revealed a porous and coiled graphite morphology that exfoliated to ultrathin sheets with wavy structures, and crumpled graphene oxide nanosheets with a morphology similar to severely wrinkled paper that rippled and entangled with each other. These photos revealed that graphene had a higher porosity and a far larger effective surface area than graphite. Electrochemical analyses using CV and EIS techniques revealed that graphene had the higher storage capacity than that ultra-thin graphite which was attributed to its large effective surface area and good ability to reactivity with the electrolyte to chemisorb Li<sup>+</sup> ions. Graphene can also facilitate charge transfer during discharge-charge actions and provide excellent rate capability. Study charge/discharge profiles at the current density of 200 mA g<sup>-1</sup> in the electrolyte of 1M LiPF<sub>6</sub> containing EMC/EC/DEC/DMC with a volume ratio of 1:1:5:2 (1M LiPF<sub>6</sub> + (EMC/EC/DEC/DMC 1:1:5:2)) as optimal stoichiometry of carbonate solvents (EC, DEC, DMC, EMC) showed that for graphite, the first-cycle discharge and charge capacities were 138 and 111 mAh g<sup>-1</sup>, respectively, and for graphene, the corresponding capacities were enhanced to 143 and 117 mAh g<sup>-1</sup> respectively. Graphene nanopores, coiled morphological edge-type sites as active defects, and increased effective surface area of graphene nanosheets as disordered carbon nanostructure give more

Li<sup>+</sup> insertion active sites, resulting in an increase in capacity. Study the galvanostatic charge-discharge and the cycling performances of graphene electrode in graphene/Li cell using 1M LiPF<sub>6</sub> containing (EMC/EC/DEC/DMC/SL 1:1:5:2:1) and (EMC/EC/DEC/DMC/FEC 1:1:5:2:1) showed that excellent specific capacity more than 124 mAh g<sup>-1</sup> and good stability over 500 cycles were obtained for electrolyte solution containing EMC/EC/DEC/DMC/SL with volume ratio of 1:1:5:2:1, and the SL-mixed solution can be employed at high potential (5.3 V vs Li/Li<sup>+</sup>).

## References

1. F.H. Gandoman, J. Jaguemont, S. Goutam, R. Gopalakrishnan, Y. Firouz, T. Kalogiannis, N. Omar and J. Van Mierlo, *Applied Energy*, 251 (2019) 113343.
2. X. Tong, F. Zhang, B. Ji, M. Sheng and Y. Tang, *Advanced Materials*, 28 (2016) 9979.
3. S. Shen, M. Sadoughi, X. Chen, M. Hong and C. Hu, *Journal of Energy Storage*, 25 (2019) 100817.
4. X. Zhang, Y. Tang, F. Zhang and C.S. Lee, *Advanced energy materials*, 6 (2016) 1502588.
5. N. Wu, X. Zhou, P. Kidkhunthod, W. Yao, T. Song and Y. Tang, *Advanced Materials*, 33 (2021) 2101788.
6. W. Zhang, L. Liang, F. Zhao, Y. Liu, L. Hou and C. Yuan, *Electrochimica Acta*, 340 (2020) 135871.
7. A. Yu, Q. Pan, M. Zhang, D. Xie and Y. Tang, *Advanced Functional Materials*, 30 (2020) 2001440.
8. K. Abraham, *ACS Energy Letters*, 5 (2020) 3544.
9. M. Yang, C. Li, Y. Zhang, D. Jia, X. Zhang, Y. Hou, R. Li and J. Wang, *International Journal of Machine Tools and Manufacture*, 122 (2017) 55.
10. H. Yuan, W. Song, M. Wang, Y. Gu and Y. Chen, *Journal of Alloys and Compounds*, 784 (2019) 1311.
11. C. Jiang, L. Xiang, S. Miao, L. Shi, D. Xie, J. Yan, Z. Zheng, X. Zhang and Y. Tang, *Advanced Materials*, 32 (2020) 1908470.
12. C. Xin, L. Changhe, D. Wenfeng, C. Yun, M. Cong, X. Xuefeng, L. Bo, W. Dazhong, H.N. LI and Y. ZHANG, *Chinese Journal of Aeronautics*, (2021) 1.
13. T. Wei, Z. Wang, M. Zhang, Q. Zhang, J. Lu, Y. Zhou, C. Sun, Z. Yu, Y. Wang and M. Qiao, *Materials Today Communications*, 31 (2022) 103518.
14. L. Tang, Y. Zhang, C. Li, Z. Zhou, X. Nie, Y. Chen, H. Cao, B. Liu, N. Zhang and Z. Said, *Chinese Journal of Mechanical Engineering*, 35 (2022) 1.
15. Y. Li, M. Vilathgamuwa, T. Farrell, N.T. Tran and J. Teague, *Electrochimica Acta*, 299 (2019) 451.
16. C. Zhao, M. Xi, J. Huo and C. He, *Physical Chemistry Chemical Physics*, 23 (2021) 23219.
17. C. Wang, N. Lu, S. Wang, Y. Cheng and B. Jiang, *Applied Sciences*, 8 (2018) 2078.
18. T. Gao, C. Li, D. Jia, Y. Zhang, M. Yang, X. Wang, H. Cao, R. Li, H.M. Ali and X. Xu, *Journal of cleaner production*, 277 (2020) 123328.
19. H. Sun, Y. Liu, Y. Yu, M. Ahmad, D. Nan and J. Zhu, *Electrochimica Acta*, 118 (2014) 1.
20. L. Sun, W. Kong, Y. Jiang, H. Wu, K. Jiang, J. Wang and S. Fan, *Journal of Materials Chemistry A*, 3 (2015) 5305.
21. V. Mani, S.-M. Chen and B.-S. Lou, *International Journal of Electrochemical Science*, 8 (2013) 11641.
22. R. Cheng, L. Sun, F. Xu, Y. Luo, C. Zhang, Y. Xia, S. Wei, Y. Guan, M. Zhao and Q. Lin, *International Journal of Electrochemical Science*, 15 (2020) 2624.

23. W. Yinwei, L. Shoufa, Z. Ning, Q. Xun and Z. Zhaofeng, *International Journal of Electrochemical Science*, 14 (2019) 618.
24. X. Fan and C. Wang, *Chemical Society Reviews*, 50 (2021) 10486.
25. W. Li, Y. Pang, J. Liu, G. Liu, Y. Wang and Y. Xia, *RSC advances*, 7 (2017) 23494.
26. A. Lewandowski and A. Świdowska-Mocek, *Journal of Power sources*, 194 (2009) 601.
27. W. Lu, L. Sun, Y. Zhao, T. Wu, L. Cong, J. Liu, Y. Liu and H. Xie, *Energy Storage Materials*, 34 (2021) 241.
28. X. Wu, C. Li, Z. Zhou, X. Nie, Y. Chen, Y. Zhang, H. Cao, B. Liu, N. Zhang and Z. Said, *The International Journal of Advanced Manufacturing Technology*, 117 (2021) 2565.
29. L. Yang, Q. Dai, L. Liu, D. Shao, K. Luo, S. Jamil, H. Liu, Z. Luo, B. Chang and X. Wang, *Ceramics International*, 46 (2020) 10917.
30. T. Gao, C. Li, Y. Wang, X. Liu, Q. An, H.N. Li, Y. Zhang, H. Cao, B. Liu and D. Wang, *Composite Structures*, 286 (2022) 115232.
31. Y. Chen, J. Long, B. Xie, Y. Kuang, X. Chen, M. Hou, J. Gao, H. Liu, Y. He and C.-P. Wong, *ACS Applied Materials & Interfaces*, 14 (2022) 4647.
32. J.-Q. Liu, Q.-C. Zhuang, Y.-L. Shi, X. Yan, X. Zhao and X. Chen, *RSC advances*, 6 (2016) 42885.
33. A.P. Cohn, L. Oakes, R. Carter, S. Chatterjee, A.S. Westover, K. Share and C.L. Pint, *Nanoscale*, 6 (2014) 4669.
34. W. Wu, X. Li and S. Kadaei, *Advances in Civil Engineering*, 2022 (2022) 1.
35. J. Kang, Y. Xue, J. Yang, Q. Hu, Q. Zhang, L. Gu, A. Selloni, L.-M. Liu and L. Guo, *Journal of the American Chemical Society*, 144 (2022) 8969.
36. W. Hao and J. Xie, *Journal of Electrochemical Energy Conversion and Storage*, 18 (2021) 1.
37. D. Jia, Y. Zhang, C. Li, M. Yang, T. Gao, Z. Said and S. Sharma, *Tribology International*, 169 (2022) 107461.
38. Y. Zhong, T. Shi, Y. Huang, S. Cheng, C. Chen, G. Liao and Z. Tang, *Nanoscale Research Letters*, 14 (2019) 85.
39. T. Gao, Y. Zhang, C. Li, Y. Wang, Y. Chen, Q. An, S. Zhang, H.N. Li, H. Cao and H.M. Ali, *Frontiers of Mechanical Engineering*, 17 (2022) 1.
40. Z. Wang, X. Yan, F. Wang, T. Xiong, M.-S. Balogun, H. Zhou and J. Deng, *Carbon*, 174 (2021) 556.
41. Z. Huang, P. Luo, H. Zheng and Z. Lyu, *Ceramics International*, 48 (2022) 18765.
42. Z. Ding, X. Qin, C. You, M. Wu, Y. He, F. Kang and B. Li, *Electrochimica Acta*, 270 (2018) 192.
43. L.-Z. Bai, D.-L. Zhao, T.-M. Zhang, W.-G. Xie, J.-M. Zhang and Z.-M. Shen, *Electrochimica Acta*, 107 (2013) 555.
44. Z. Said, S. Arora, S. Farooq, L.S. Sundar, C. Li and A. Allouhi, *Solar Energy Materials and Solar Cells*, 236 (2022) 111504.
45. L. Zhang, L. Chen, H. Luo, X. Zhou and Z. Liu, *Advanced Energy Materials*, 7 (2017) 1700034.
46. Y. Xu, X. Chen, H. Zhang, F. Yang, L. Tong, Y. Yang, D. Yan, A. Yang, M. Yu and Z. Liu, *International Journal of Energy Research*, (2022) 1.
47. H. Fan, L. Qi, M. Yoshio and H. Wang, *Solid State Ionics*, 304 (2017) 107.
48. D. Zhu and H. Wang, *Langmuir*, 37 (2021) 10797.
49. X. Cui, C. Li, Y. Zhang, Z. Said, S. Debnath, S. Sharma, H.M. Ali, M. Yang, T. Gao and R. Li, *Journal of Manufacturing Processes*, 80 (2022) 273.
50. L. Lombardo, S. Brutti, M.A. Navarra, S. Panero and P. Reale, *Journal of Power Sources*, 227 (2013) 8.
51. J. Saunier, F. Alloin, J.-Y. Sanchez and G. Caillon, *Journal of power sources*, 119 (2003) 454.

52. K. Hayashi, Y. Nemoto, S.-i. Tobishima and J.-i. Yamaki, *Electrochimica Acta*, 44 (1999) 2337.
53. X. Wang, C. Li, Y. Zhang, H.M. Ali, S. Sharma, R. Li, M. Yang, Z. Said and X. Liu, *Tribology International*, 174 (2022) 107766.
54. T. Zhang, F. Zhang, L. Zhang, Y. Lu, Y. Zhang, X. Yang, Y. Ma and Y. Huang, *Carbon*, 92 (2015) 106.
55. A. Heckmann, J. Thienenkamp, K. Beltrop, M. Winter, G. Brunklaus and T. Placke, *Electrochimica acta*, 260 (2018) 514.
56. S.T. Yang, X.Y. Li, T.L. Yu, J. Wang, H. Fang, F. Nie, B. He, L. Zhao, W.M. Lü and S.S. Yan, *Advanced Functional Materials*, 32 (2022) 2202366.
57. S.C. Jung, Y.-J. Kang, D.-J. Yoo, J.W. Choi and Y.-K. Han, *The Journal of Physical Chemistry C*, 120 (2016) 13384.
58. M. Yang, C. Li, Y. Zhang, Y. Wang, B. Li, D. Jia, Y. Hou and R. Li, *Applied Thermal Engineering*, 126 (2017) 525.
59. S. Zhang, T. Jow, K. Amine and G. Henriksen, *Journal of Power Sources*, 107 (2002) 18.
60. Z. Zhang, X. Chen, F. Li, Y. Lai, J. Li, P. Liu and X. Wang, *Journal of Power Sources*, 195 (2010) 7397.
61. P. Murmann, P. Niehoff, R. Schmitz, S. Nowak, H. Gores, N. Ignatiev, P. Sartori, M. Winter and R. Schmitz, *Electrochimica Acta*, 114 (2013) 658.